Simulation Modelling Practice and Theory 18 (2010) 910–925

Contents lists available at ScienceDirect

Simulation Modelling Practice and Theory

journal homepage: www.elsevier.com/locate/simpat

Modeling and simulation of the market fluctuations by the finite range contact systems

Junhuan Zhang, Jun Wang *

Institute of Financial Mathematics and Financial Engineering, College of Science, Beijing Jiaotong University, Beijing 100044, PR China

ARTICLE INFO

Article history:
Received 11 August 2009
Received in revised form 9 February 2010
Accepted 13 February 2010
Available online 19 February 2010

Keywords:
Econophysics
Stock index
Finite range contact model
Probability distribution
Returns
Computer simulation
Statistical analysis

ABSTRACT

In this paper, we model a new random stock price model for the stock markets based on the finite range contact process, which is a model for epidemic spreading that mimics the interplay of local infections and recovery of individuals, it is a member of a class of stochastic processes known as interacting particle systems. Then, we analyze the statistical behaviors of Shanghai Stock Exchange (SSE) Composite Index, Shenzhen Stock Exchange (SZSE) Composite Index, Dow Jones Industrial Average Index (DJIA), Nasdaq Composite Index (IXIC), the standard and Poor's 500 Index (S&P500) and the simulative data derived from the finite range contact model by comparison. And six individual Chinese stocks from large-cap, mid-cap and small-cap categories are discussed. Furthermore, we investigate the long range correlations of the returns for these indices and the corresponding simulative data by applying the detrended fluctuation analysis. At last, the positive part of the probability distributions of the logarithmic returns for the actual data and the simulative data are studied by the q-Gaussian dynamic systems. The main objective of this work is to discuss the impact on the returns with the different range financial models.

1. Introduction

The contact process, a model for epidemic spreading in a continuous time Markov process, is a member of a class of stochastic processes known as interacting particle systems, see [13,14]. One interpretation of the contact process, is often thought of as a crude model for the spread of a disease or a biological population. Healthy individuals become infected at a rate which proportional to the number of the infected neighbors, and infected individuals recover at a constant rate. Specifically speaking, the contact model is a continuous time Markov process η_s in the configuration $\{0,1\}^{Z^d}$. If $\eta_s(x) = 1$, one individual at the point is regarded as infected and recovers from its infection at rate one; if $\eta_s(x) = 0$, the individual at the point x is healthy and will be infected at a rate equal to λ times the number of the infected neighbors. In the contact systems, the nearest neighbor contact process has been studied deeply in the past work. There also has been some research work done in generalizing the contact process in various ways to conclude the finite range and the long range contact process, see [2,13,14].

Some work has been done by applying the stochastic interacting particle systems to study the behavior of fluctuation of stock prices in a stock market. Stauffer and Jan [17,18] gave a price changes model by the lattice percolation theory, in the local interaction of percolation, the local interaction or influence among traders in one stock market is modeled, and a cluster of percolation is used to define the cluster of traders sharing the same investment attitude towards to the market. Let p_c

* Corresponding author. Tel./fax: +86 10 51682867.
E-mail address: wangjun@bjtu.edu.cn (J. Wang).

1569-190X/$ - see front matter © 2010 Elsevier B.V. All rights reserved.
doi:10.1016/j.simpat.2010.02.008

denote the critical value of influence rate in percolation model, around or at this critical value, applying the results of percolation clusters [17,18], show the existence of fat-tails for the stock returns. Here, the critical phenomena of percolation model is used to illustrate the herd behavior of stock market participants. In their study, they assume that the information in the stock market leads to the stock price fluctuation and the investors in stock market follow the effect of sheep flock. There are also some work that has been done by applying Ising type models to a financial model, see [7,9]. In the present paper, we apply the finite range contact systems to study the fluctuation phenomena of stock indices, and we hope that this work is useful for understanding the statistical behaviors of fluctuations in the globalized securities markets. First, we will discuss the statistical behavior, the fat-tails phenomena, the power-law distributions of the actual data and the simulation data. Then, we investigate the long range correlations of the return processes by the detrended fluctuation analysis (DFA) through the computer simulation on the financial model. At last, the positive part of the probability distributions of logarithmic returns for the actual data and the simulation data are studied by a dynamic model.

In the present paper, the actual data of five stocks indices all over the world are analyzed. The daily data of SSE composite index, which is one of the most important security indices in China for the 12-year period from January 2nd 1997 to August 11th 2009, the total number of observed data is 3042. The daily data of SZSE composite index from January 2nd 1997 to August 11th 2009, the total number of observed data is about 3046. Another database is the standard and Poor's 500 index (S&P500), the daily data for 19-year period from January 2nd 1990 to July 17th 2009, and the total number of observed data is 4783. And we also study Dow Jones industrial average index (DJIA), the sample daily data is January 2nd 1990 to July 17th 2009 (the total data number is about 4958). In addition, the daily data of Nasdaq composite index (IXIC), its daily data is from September 2nd 1996 to July 17th 2009, the data size is 3208 in total.

Furthermore, we study six individual Chinese stocks from large-cap, mid-cap and small-cap categories according to the market capitalization on November 5th 2009. The large-cap categories are Daqin Railway (DQTL) and China Railway Construction Corporation (CRCC) from March 10th 2008 to November 5th 2009. The mid-cap categories are Shanghai Bailian Group (BLGF) and Yuyuan Tourist Mart (YYTM) from January 2nd 2004 to November 5th 2009. The small-cap categories are Anxin trust and investment (AXXT) and Shaanxi international trust and investment (SITI) from January 4th 2000 to November 5th 2009. At the same time, we also investigate the simulation data derived from the finite range contact model, the number of simulation data from the financial model is about 5000.

2. Description of the finite range contact model

In the above section, we give a brief description for the contact model, next we introduce the mathematical description of the process. The finite range contact model on $\mathbb{z}^d$ with infection parameter λ is a continuous time Markov process η_s on the configuration space $\{0,1\}^{\mathbb{z}^d}$. A configuration $\eta \in \{0,1\}^{\mathbb{z}^d}$ is often be identified with subsets A of $\mathbb{z}^d$ via $A = \{x \in \mathbb{z}^d : \ \eta(x) = 1\}$. Individuals in A are regarded as infected, while the other individuals are thought of as being healthy. The transition rates for η_s are given by

(a) $A \to A \setminus \{x\}$ for all $x \in A$ at rate 1, and
(b) $A \to A \cup \{x\}$ for all $x \notin A$ at rate $\lambda|\{y \in A : \ |y - x| \leqslant R\}|$

where R is the range of the model, $|A|$ denote the cardinality of a finite set A, and $|y - x|$ is the minimal length of a path from x to y. More formally, the connection between the rate function $c(x,\eta)$ and the process η_s is made through the generator Ω of η_s. For functions f on $\{0,1\}^{\mathbb{z}^d}$ that depend on finitely many coordinates, the generator has the form

$$\Omega f(\eta) = \sum_x c(x,\eta)[f(\eta^x) - f(\eta)]$$

where $\eta^x(y) = \eta(y)$ if $y \neq x, \eta^x(y) = -\eta(y)$ if $y = x$, for $x, y \in \mathbb{Z}^d$. And $c(x,\eta)$ is given by (see [12,13])

$$c(x,\eta) = \begin{cases} 1 & \text{if } \eta(x) = 1, \\ \lambda \sum\limits_{y:|y-x|\leqslant R} \eta(y) & \text{if } \eta(x) = 0. \end{cases}$$

Let η_s^A denote the state at time s with the initial state $\eta_0^A = A$. More generally, we consider the initial distribution as v_θ, the product measure with density θ, that is, each site is independently occupied with probability θ and let η_s^θ to denote the contact model with initial distribution v_θ. Further let $\eta_s^{\{0\}}(x)$ be the state of $x \in \mathbb{Z}^d$ at time s with the initial point $\{0\}$. The most important feature of the contact process is that survival and extinction can be both occur, which of these occurs depends on the value of λ. There is a critical value λ_c, if $\lambda < \lambda_c$, the contact process is said to die out or become extinct, that is

$$P(\eta_s^{\{0\}} \neq \emptyset, \ \text{forall } s \geqslant 0) = 0;$$

otherwise (for $\lambda > \lambda_c$) it is said to survive.

For simplicity, we introduce the graphical representation of the one-dimensional finite range contact model with the configuration space $\{0,1\}^{\mathbb{Z}}$, the graphical representation is very helpful to for us to illustrate and simulate the model. We

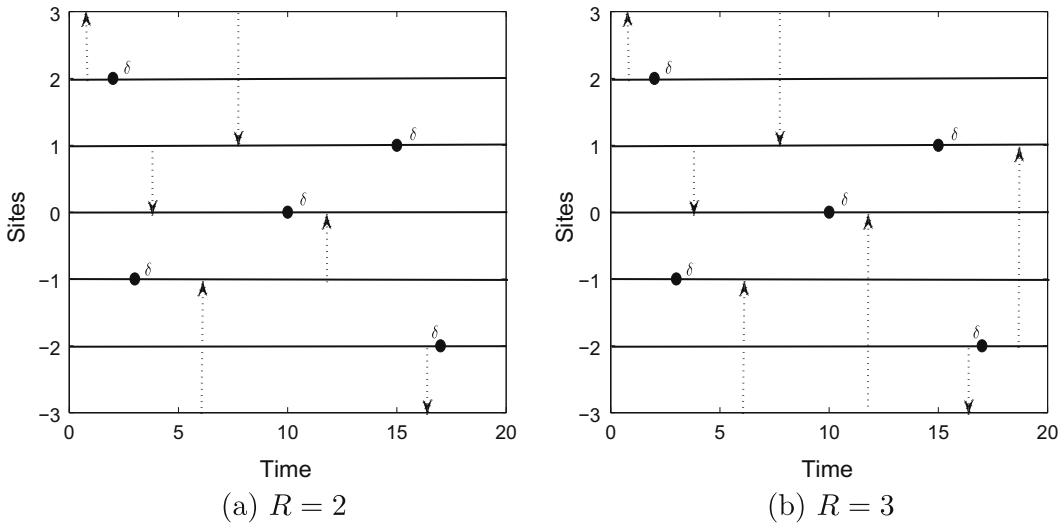

Fig. 1. (a) The graphical representation of one-dimensional contact model with the range $R = 2$. The y-axis is the sites and the x-axis is the time. (b) The graphical representation of one-dimensional contact model with the range $R = 3$.

consider $\mathbb{R}_+ \times \mathbb{Z}$ as the space-time. For each pair $y, \tilde{y} \in \mathbb{Z}$ with $|y - \tilde{y}| \leqslant R$, let $\left\{T_n^{(y,\tilde{y})}, n \geqslant 1\right\}$ a Poisson process with a rate λ, and let $\{U_n^y, n \geqslant 1\}$ a Poisson process with a rate one. Along each time line $\mathbb{R}_+ \times \{y\}$, we place points according to a Poisson process with intensity 1, independently of the other time lines, and at points' times U_n^y, we put a δ at y. The effect of a δ is to recover the individual at y (if one is infected). For each ordered pair of distinct time lines from $\mathbb{R}_+ \times \{y\}$ to $\mathbb{R}_+ \times \{\tilde{y}\}$ (where $|y - \tilde{y}| \leqslant R$), we place directed arrows at times $T_n^{(y,\tilde{y})}$ from y to $\tilde{y}$, according to a Poisson process with intensity λ, independently of the other Poisson processes, this indicates that if y is infected then $\tilde{y}$ will become infected (if it is not already), see [8,13,14]. Then, the construction of graphical representation for one-dimensional contact model is given in Fig. 1. To construct the process from this "graphical representation", we imagine fluid entering the left side at the points in η_0 (at time 0) and flowing right the structure. The $\delta's$ are the dams and the arrows are pipes which allow the fluid to flow in the indicated direction.

Recently, some research work has been made by applying the concepts and methods of statistical physics to study economic problems, sometimes it is called 'econophysics', see [7,9,11,15–18]. The finite range contact model is a statistic physical system comprised of a large number of interacting units which is similar to financial markets consisting of a large number of interacting 'agents'. There are stochasticity or random behaviors ingrained in the finite contact model, which considers financial markets as a complicated evolving system. The motivation of modeling stock price by using a finite range contact model is to uncover the empirical laws in stock price and understand better the dynamics of financial systems, see [16]. Through the comparisons between the real markets and the financial model, we hope to show that the financial model of the present paper is reasonable to some extent.

For any large positive integer $L \geqslant 1$, let ${}_L\eta_s$ be the truncated contact process defined via the graphical representation, but using only paths with vertical segments corresponding to sites in $(-L, -L)^d$ and infection arrows from $(x, \cdot)$ to $(y, \cdot)$ with $x \in (-L, -L)^d$. Then, for every finite A and every constant $C \geqslant 1$, we have (see [14])

$$\lim_{s\to\infty} \lim_{L\to\infty} P\left(|{}_L\eta_s^A| \geqslant C\right) = P\left(\eta_s^A \neq \emptyset, \text{ forall } s \geqslant 0\right).$$

Here we introduce the truncated contact process, because the number of investors is finite (although it is large enough). The above limit implies that applying the finite range contact system to a stock market is reasonable.

3. Modeling a price model for a stock market

Throughout this section, we adopt the setting and notation of Sections 1 and 2. The analysis of market indices and returns is an active topic to understand and model the distribution of financial price fluctuations, which has long been a focus of economic research, see [1–7,9,11,12,15,17–19]. The main objective of this section is to construct the return process of stock prices on R-range integer lattice by applying the finite range contact model. In this paper, we also assume that the stock price fluctuation results from the investors' investment attitudes towards to the stock market, and suppose that the investment attitude is represented by the viruses of the finite range contact model, which accordingly classify buying stock, selling stock and holding stock.

Consider a model of auctions for a stock in a stock market. Assume that each trader can trade the stock several times at each day $t \in \{1, 2, \ldots, N\}$, but at most one unit number of the stock at each time. Let l be the time length of trading time in

each trading day, we denote the stock price at time s in the tth trading day by $P_t(s)$, where $s \in [0, l]$. Suppose that this stock consists of $n+1$ (n is large enough) investors, who are located in a line $\{-n/2, \ldots, -1, 0, 1, \ldots, n/2\} \subset \mathbb{Z}$ (similarly for d-dimensional lattice $\mathbb{Z}^d$). At the beginning of trading in each day, suppose that the investors (with the initial distribution ν_θ, see the definition of η_s^θ in Section 2) receive some news. We define a random variable $\xi_t(\theta)$ for these investors, suppose that these investors taking buying positions ($\xi_t(\theta) = 1$), selling positions ($\xi_t(\theta) = -1$) or neutral positions ($\xi_t(\theta) = 0$) with probability p_1, p_{-1} or $1 - (p_1 + p_{-1})$, respectively. Then these investors send bullish, bearish or neutral signal to their neighbors. According to d-dimensional contact dynamic system, investors can affect each other or the news can be spread, which is assumed as the main factor of price fluctuations. Moreover, here the investors can change their buying positions or selling positions to neutral positions independently at a constant rate. More specifically, (i) When $\xi_t(\theta) = 1$ and if $\eta_s^\theta(x) = 1$, we say that the investor at x takes buying position at time s, and this investor recovers to neutral position 0 at rate 1; if $\eta_s^\theta(x) = 0$, we think the investor at x takes neutral position at time s, and this investor is changed to take buying position by his neighbors at rate $\lambda \sum_{y:|y-x| \leqslant R} \eta_s^\theta(y)$. In this case, the more investors with taking buying positions, the more possible the stock price goes up. (ii) When $\xi_t(\theta) = -1$ and if $\eta_s^\theta(x) = 1$, we say that the investor at x takes selling position at time s, also this investor recovers to neutral position 0 at rate 1; if $\eta_s^\theta(x) = 0$, the investor is changed to take selling position by his neighbors at rate $\lambda \sum_{y:|y-x| \leqslant R} \eta_s^\theta(y)$. (iii) When the initial random variable $\xi_t(\theta) = 0$, the process $\eta_s^\theta(x)$ is ignored, this means that the investors do not affect the fluctuation of the stock price.

For a fixed $s \in [0, l]$ (l large enough), let

$$B_t(s) = \xi_t(\theta)|\eta_s^\theta|/n, \quad s \in [0, l]$$

where n depends on the trading days N. From the above definitions and [1,10,20], we define the stock price at tth trading day $t (t = 1, 2, \ldots, N)$ as

$$P_t(s) = e^{\alpha B_t(s)} P_{t-1}(s), \quad s \in [0, l]$$

where $\alpha > 0$, represents the depth parameter of the market. Then we have

$$P_t(s) = P_0 \exp\left\{\alpha \sum_{k=1}^{t} B_k(s)\right\}, \quad s \in [0, l]$$

where P_0 is the initial stock price at time 0. The formula of the single-period stock logarithmic returns from t to $t+1$ is given as follows

$$r(t) = \ln P_{t+1}(s) - \ln P_t(s), \quad t = 1, 2, \ldots, N.$$

In this paper, we analyze the logarithmic returns for the daily price changes. In the light of the theory of the contact process and the above definitions, if $\lambda > \lambda_c$, the virus will not die out, namely, the news will spread widely, so this will affect the investors' positions, and finally will affect the fluctuation of the stock price. If $\lambda \leqslant \lambda_c$, the virus will die out at last, namely, the influence on the stock price by the investors is limited. In the followings, we let $s = 2000$, then the time series of the stock

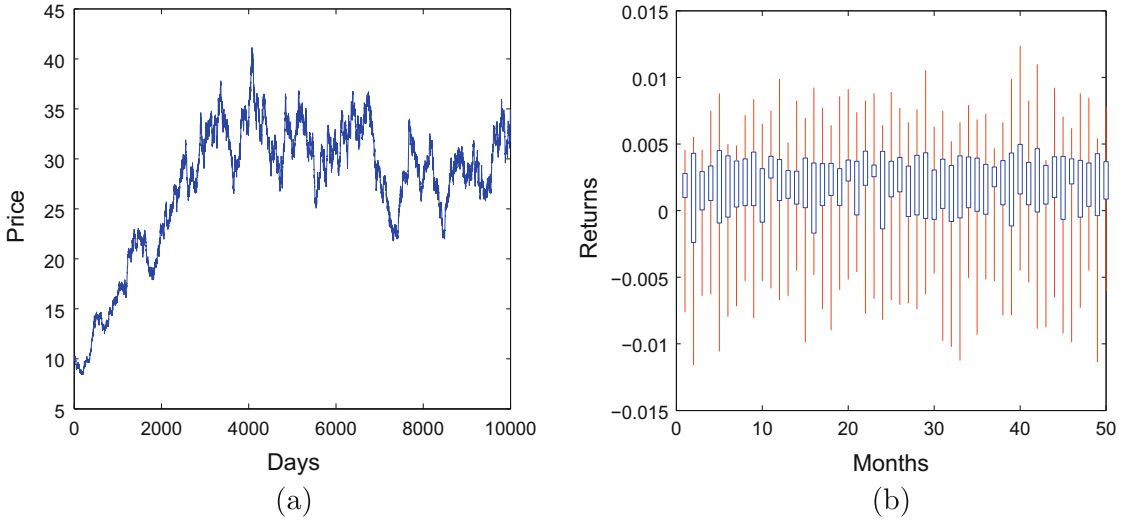

Fig. 2. Time series of the simulation data. (a) The price time series. (b) The monthly candle-chart of the corresponding returns.

prices and the monthly candle-chart of the corresponding returns by simulating the one-dimensional finite range contact model ($R = 2$) are plotted in Fig. 2, where the monthly candle-chart shows the max, min, standard deviation and medium values of the corresponding returns.

4. Statistical behaviors of the simulation for the financial price model

Our main objective in this section is to discuss and study the statistical behaviors of the logarithmic returns for the simulative data derived from the finite range contact model. Firstly, we discuss the parameter settings and comparison for the price model. Then, four parameters are discussed in the financial price model which given in Section 3, which are the intensity λ, the range of the model R, the number of investors or individuals n, and the initial density θ. For the different values of one parameter in the model, we study the trend of stock market fluctuations. Further, by the computer computations and the corresponding plots, we compare the statistical properties of the returns of the five indices with those of the financial model. In the end, we study statistical behaviors of six individual Chinese stocks from large-cap (DQTL, CRCC), mid-cap (YYTM, BLGF) and small-cap (AXXT, SITI) categories. Also, we analyze the statistical properties of the actual data (SSE composite index, SZSE composite index, DJIA, IXIC, S&P500) during the financial crisis period from September 2008 to August 2009.

4.1. Parameter setting and comparison for the price model

The parameter setting of the financial model is discussed in the present paper, and 3000 replications for the simulation are made. In this subsection, for $R = 1$, we discuss the parameter settings of the financial model. The statistics of returns for different values of parameters is given in 84 samples of Table 1, and the probability behaviors of the kurtosis and the skewness are studied. Kurtosis is a measure of the 'peakedness' of the probability distribution of a real-valued random variable. Higher kurtosis means more of the variance is due to infrequent extreme deviations, as opposed to frequent modestly sized deviations. It is known that the kurtosis of the Gaussian distribution is 3, while the kurtosis of the real markets is usually lager than 3 by the empirical research. The recent research shows that returns on the financial markets are not Gaussian, but exhibit the excess kurtosis and the fatter tails than the normal distribution, which is usually called the 'fat-tail' phenomenon, see [3,4,6,11,15–18].

By the computer simulations, Table 1 gives a description of the statistics for the price model with the range $R = 1$. For example, the number of kurtosis values which are larger than 3 is nine times among the twelve tests for $\lambda = 10$. Considering the kurtosis values for different values λ in Table 1 and the kurtosis values for the real markets, most of computer simulations in the present paper are made on the parameter $\lambda = 10$. This shows that the distribution of the returns deviates from the Gaussian distribution, and the kurtosis distribution of the returns has a sharper peak and longer, fatter tails. This property is similar to the actual data distribution to some degree. Similar to Table 1, we have considered the statistical properties of returns for the financial model with the range $R = 2, 3$, and the corresponding simulations show the similar results.

Next we compare the computer simulations between the price model of the present paper and the stock price modeled by a geometric Brownian motion. Monte Carlo simulation based on Wiener process or Markov–Chain Monte Carlo simulation is one of the common simulation ways that is widely used in financial institutes, here we give a Table 2 to show the statistics of returns for the geometric Brownian motion price model.

Assuming that the behavior of the stock price is determined by the following stochastic differential equation

$$dS_t = S_t(\mu dt + \sigma dW_t)$$

where μ and σ are two constants, and $\{W_t\}$ is a standard Brownian motion. And the above equation has a closed-from solution

$$S_t = S_0 \exp\{(\mu - \sigma^2/2)t + \sigma W_t\}$$

where S_0 is the starting price at time 0, see [1,10,20]. This price model following the geometric Brownian motion was suggested by Black and Scholes [1], sometimes it is also called the Black–Scholes model.

We simulate 3000 replications for different values of μ and σ by computer, where $S_0 = 1000$, and the data size of the simulation is 5000. The statistics of returns for the simulation is given in Table 2. By the comparisons between Tables 1 and 2, we find that the number of kurtosis values which are larger than 3 is 49 in 84 replications for the financial model, while that of Monte Carlo simulation is 42 in 84 replications (where 24 replications are given in Table 2) for the geometric Brownian motion. From this view, we think that the financial model of this paper is reasonable for the real stock market to some extent.

Remark. In the above work, the parameters μ and σ are selected by $\mu \in \{0.05, 0.1, 0.15, 0.2, 0.25, 0.3, 0.35\}$ and $\sigma \in \{0.1, 0.11, 0.12, 0.13, 0.14, 0.15, 0.16, 0.17, 0.18, 0.19, 0.20, 0.21\}$. In order to investigate the problem whether the similarity may depend on the chosen of numerical combinations, we consider other pairs of (μ, σ) in Black–Scholes model. Let $\mu \in \{0.5, 0.55, 0.6, 0.65, 0.7, 0.75, 0.8\}$ and $\sigma \in \{0.1, 0.11, 0.12, 0.13, 0.14, 0.15, 0.16, 0.17, 0.18, 0.19, 0.20, 0.21\}$. Then we do the similar empirical research as the above, the empirical result reveals that the number of kurtosis values which are larger than 3 is 43 in 84 replications for Black–Scholes model. This shows that, the similarity of the financial model and the geometric Brownian motion can hold when the numerical combinations (μ, σ) do not change greatly.

Table 1
The parameter settings of returns for the financial price model.

R	λ	n	θ	Kurtosis	Skewness	Variance	Mean	Max	Min
1	2	100	0.05	2.9168	−0.0427	4.0181e−006	−2.7583e−005	0.0065	−0.0071
1	2	100	0.1	3.0392	−1.5882e−004	9.0316e−006	−3.1055e−005	0.0100	−0.0121
1	2	100	0.15	3.0199	−0.0303	3.9098e−006	5.6025e−007	0.0067	−0.0075
1	2	200	0.05	3.0219	0.0338	2.4426e−006	1.9302e−005	0.0061	−0.0059
1	2	200	0.1	2.9320	−0.0464	4.4632e−006	−1.7162e−005	0.0076	−0.0075
1	2	200	0.15	3.0087	0.0150	6.0393e−006	1.6377e−007	0.0089	−0.0086
1	2	300	0.05	3.0065	−0.0065	1.4874e−006	9.0883e−006	0.0042	−0.0057
1	2	300	0.1	2.9291	0.0324	2.9785e−006	−5.0428e−006	0.0061	−0.0062
1	2	300	0.15	3.0199	−0.0303	3.9098e−006	5.6025e−007	0.0067	−0.0075
1	2	400	0.05	2.8932	0.0110	1.1687e−006	1.3234e−005	0.0038	−0.0038
1	2	400	0.1	2.9352	0.0040	2.2046e−006	3.0071e−005	0.0050	−0.0054
1	2	400	0.15	3.0772	−0.0325	2.9957e−006	−8.2809e−006	0.0068	−0.0064
1	4	100	0.05	2.9385	−0.0663	1.0147e−005	−1.1019e−004	0.0109	−0.0107
1	4	100	0.1	3.0614	0.0026	2.2237e−005	−8.9576e−005	0.0174	−0.0181
1	4	100	0.15	2.9617	−0.0066	8.4191e−006	−8.5042e−006	0.0094	−0.0105
1	4	200	0.05	3.0008	−0.0639	6.0053e−006	4.2255e−005	0.0087	−0.0109
1	4	200	0.1	3.0002	0.0278	1.0325e−005	−3.8292e−006	0.0119	−0.0118
1	4	200	0.15	3.0176	0.0025	1.3688e−005	−4.0734e−005	0.0135	−0.0139
1	4	300	0.05	2.8262	−0.0396	3.8503e−006	3.8823e−006	0.0065	−0.0066
1	4	300	0.1	2.9796	−0.0582	7.2449e−006	1.9953e−005	0.0085	−0.0092
1	4	300	0.15	2.9617	−0.0066	8.4191e−006	−8.5042e−006	0.0094	−0.0105
1	4	400	0.05	2.9906	0.0243	2.8682e−006	−2.1397e−006	0.0064	−0.0059
1	4	400	0.1	2.9581	0.0448	5.0148e−006	−5.8663e−005	0.0097	−0.0078
1	4	400	0.15	2.8556	0.0180	6.4861e−006	−5.1278e−006	0.0081	−0.0085
1	6	100	0.05	3.0176	−0.0065	1.7132e−005	−7.2458e−005	0.0148	−0.0148
1	6	100	0.1	2.9021	−0.0538	1.0426e−005	−9.4251e−005	0.0119	−0.0122
1	6	100	0.15	3.0559	−0.0267	1.2066e−005	5.0653e−005	0.0132	−0.0130
1	6	200	0.05	2.9566	−0.0230	9.8975e−006	−3.8672e−005	0.0119	−0.0116
1	6	200	0.1	3.0288	−0.0637	1.5692e−005	−1.6958e−006	0.0139	−0.0146
1	6	200	0.15	3.1076	−0.0102	1.7719e−005	−6.9571e−005	0.0145	−0.0160
1	6	300	0.05	3.1511	−0.0529	6.2067e−006	1.5958e−005	0.0100	−0.0086
1	6	300	0.1	2.9021	−0.0538	1.0426e−005	−9.4251e−005	0.0119	−0.0122
1	6	300	0.15	3.0559	−0.0267	1.2066e−005	5.0653e−005	0.0132	−0.0130
1	6	400	0.05	3.0160	−0.0042	4.8690e−006	7.4556e−005	0.0080	−0.0075
1	6	400	0.1	2.9815	0.0040	8.2364e−006	−2.0985e−005	0.0127	−0.0093
1	6	400	0.15	3.0419	−0.0471	9.0170e−006	4.8726e−005	0.0119	−0.0103
1	8	100	0.05	3.0181	−0.0578	2.4761e−005	7.4314e−006	0.0187	−0.0167
1	8	100	0.1	2.9719	−0.0368	4.3639e−005	−2.3934e−004	0.0213	−0.0258
1	8	100	0.15	2.9278	−0.1039	4.5537e−005	−1.1192e−004	0.0239	−0.0253
1	8	200	0.05	3.0549	−0.0579	1.4336e−005	−1.4495e−005	0.0130	−0.0151
1	8	200	0.1	3.0831	−0.0065	2.2582e−005	−1.1305e−004	0.0169	−0.0200
1	8	200	0.15	3.1366	−0.0537	2.2859e−005	−5.2554e−005	0.0182	−0.0193
1	8	300	0.05	2.9808	−0.0040	9.2560e−006	−3.8016e−005	0.0100	−0.0108
1	8	300	0.1	2.9543	0.0081	1.5081e−005	−6.4924e−005	0.0139	−0.0139
1	8	300	0.15	2.9638	−0.0536	1.4381e−005	−2.8006e−005	0.0140	−0.0156
1	8	400	0.05	2.9247	0.0042	7.4335e−006	−2.6859e−005	0.0101	−0.0092
1	8	400	0.1	2.9766	−0.0295	1.1146e−005	2.0488e−005	0.0114	−0.0122
1	8	400	0.15	3.0437	0.0174	1.1214e−005	−1.7630e−005	0.0124	−0.0117
1	10	100	0.05	2.9495	−0.0804	3.3003e−005	8.0114e−005	0.0191	−0.0224
1	10	100	0.1	3.0037	−0.0641	5.3155e−005	−2.1873e−004	0.0269	−0.0287
1	10	100	0.15	2.9680	−0.0314	4.7037e−005	2.3791e−005	0.0248	−0.0248
1	10	200	0.05	3.1354	−0.0315	2.0227e−005	−6.9287e−005	0.0213	−0.0162
1	10	200	0.1	3.0537	−0.0401	2.7680e−005	6.6381e−006	0.0202	−0.0193
1	10	200	0.15	3.0320	−0.0016	2.3227e−005	6.2900e−005	0.0159	−0.0179
1	10	300	0.05	3.0288	−0.0403	1.2595e−005	9.5553e−005	0.0123	−0.0117
1	10	300	0.1	3.1316	−0.0028	1.7962e−005	−7.4780e−005	0.0184	−0.0159
1	10	300	0.15	3.0760	−0.0469	1.5472e−005	5.0099e−006	0.0138	−0.0186
1	10	400	0.05	2.9548	0.0217	9.9979e−006	−4.5374e−005	0.0116	−0.0101
1	10	400	0.1	3.5992	−0.0513	1.3476e−005	−2.5957e−005	0.0123	−0.0148
1	10	400	0.15	3.1065	−0.0172	1.1499e−005	2.8713e−006	0.0131	−0.0121
1	12	100	0.05	2.8225	−0.0761	4.2747e−005	1.0715e−004	0.0235	−0.0233
1	12	100	0.1	2.9705	−0.0762	5.8582e−005	−5.9489e−005	0.0261	−0.0282
1	12	100	0.15	3.1855	−0.0329	4.4483e−005	−7.3323e−005	0.0243	−0.0248
1	12	200	0.05	3.1250	−0.0584	2.6235e−005	−6.0622e−005	0.0174	−0.0202
1	12	200	0.1	2.9714	−0.0816	2.8671e−005	3.0249e−005	0.0189	−0.0217
1	12	200	0.15	2.9869	−0.0322	2.1723e−005	−2.1238e−005	0.0180	−0.0179
1	12	300	0.05	3.0175	−0.0415	1.6687e−005	7.4791e−005	0.0143	−0.0168
1	12	300	0.1	3.0136	−0.0539	2.1118e−005	−3.2132e−005	0.0146	−0.0181

(*continued on next page*)

Table 1 (*continued*)

R	λ	n	θ	Kurtosis	Skewness	Variance	Mean	Max	Min
1	12	300	0.15	2.9581	−0.0383	1.5288e−005	4.0415e−005	0.0133	−0.0139
1	12	400	0.05	3.0886	−0.0223	1.2920e−005	−1.1666e−004	0.0143	−0.0130
1	12	400	0.1	2.9345	−0.0153	1.6409e−005	6.4893e−005	0.0161	−0.0158
1	12	400	0.15	2.9874	−0.0456	1.1657e−005	−5.6300e−006	0.0119	−0.0126
1	20	100	0.05	2.8417	−0.0709	8.6218e−005	−2.1632e−004	0.0373	−0.0373
1	20	100	0.1	3.8194	−0.0991	3.9305e−005	6.9464e−005	0.0213	−0.0287
1	20	100	0.15	5.9930	0.0624	1.4674e−005	3.8852e−005	0.0182	−0.0176
1	20	200	0.05	2.9913	−0.0376	4.9095e−005	−1.7396e−005	0.0232	−0.0238
1	20	200	0.1	3.2577	−0.0858	2.7526e−005	7.0308e−006	0.0200	−0.0231
1	20	200	0.15	4.7226	0.0943	1.0084e−005	1.5101e−005	0.0148	−0.0151
1	20	300	0.05	2.9875	−0.0286	3.3108e−005	−3.9815e−005	0.0185	−0.0200
1	20	300	0.1	3.2067	−0.0030	2.0168e−005	−9.0513e−005	0.0175	−0.0168
1	20	300	0.15	3.9085	−0.0264	8.2392e−006	1.1512e−004	0.0120	−0.0117
1	20	400	0.05	2.9671	−0.0582	2.4430e−005	4.7558e−005	0.0157	−0.0172
1	20	400	0.1	3.3568	−0.0684	1.6064e−005	−1.7888e−005	0.0151	−0.0159
1	20	400	0.15	3.5985	−0.0711	6.3421e−006	−6.3884e−005	0.0098	−0.0097

Table 2
The statistics of returns for Monte Carlo simulation.

μ	σ	Kurtosis	Skewness	Variance	Mean	Max	Min
0.05	0.10	3.1085	0.0125	1.9038e−006	5.2196e−005	0.0053	−0.0058
0.05	0.11	2.9806	−0.0165	2.2458e−006	2.9636e−005	0.0051	−0.0051
0.05	0.12	2.9298	−0.0018	2.7030e−006	2.1672e−005	0.0060	−0.0056
0.05	0.13	3.0689	0.0332	3.2225e−006	3.2460e−005	0.0079	−0.0063
0.05	0.14	3.0249	−0.0370	3.6868e−006	3.7010e−005	0.0068	−0.0080
0.05	0.15	2.9108	−0.0324	4.2151e−006	−1.6658e−005	0.0077	−0.0075
0.10	0.10	2.9965	0.0302	1.9035e−006	2.8899e−005	0.0055	−0.0047
0.10	0.11	3.0208	0.0135	2.1759e−006	1.7424e−005	0.0053	−0.0056
0.10	0.12	2.8882	−0.0330	2.7351e−006	4.3704e−005	0.0055	−0.0063
0.10	0.13	2.9965	0.0302	3.2169e−006	2.3693e−005	0.0071	−0.0061
0.10	0.14	3.0208	0.0135	3.5247e−006	9.4198e−006	0.0067	−0.0071
0.10	0.15	2.9806	−0.0165	4.1761e−006	5.2928e−005	0.0070	−0.0070
0.15	0.10	2.9503	0.0427	1.8715e−006	4.3120e−005	0.0048	−0.0049
0.15	0.11	2.8348	0.0305	2.3378e−006	5.2901e−005	0.0050	−0.0058
0.15	0.12	3.0203	−0.0032	2.7223e−006	6.4916e−005	0.0068	−0.0063
0.15	0.13	2.9503	0.0427	3.1628e−006	3.5666e−005	0.0062	−0.0064
0.15	0.14	2.8348	0.0305	3.7869e−006	4.8650e−005	0.0063	−0.0074
0.15	0.15	3.0203	−0.0032	4.2536e−006	6.3882e−005	0.0084	−0.0080
0.20	0.10	2.9376	0.0450	1.8499e−006	6.3499e−005	0.0048	−0.0047
0.20	0.11	3.0337	0.0028	2.3328e−006	9.7381e−005	0.0067	−0.0052
0.20	0.12	2.9261	−0.0490	2.7352e−006	9.8824e−005	0.0056	−0.0057
0.20	0.13	2.9376	0.0450	3.1264e−006	5.5645e−005	0.0062	−0.0062
0.20	0.14	3.0337	0.0028	3.7787e−006	9.9339e−005	0.0086	−0.0066
0.20	0.15	2.9261	−0.0490	4.2738e−006	1.0084e−004	0.0070	−0.0072

4.2. Behaviors of returns for the five indices and the financial price model

Firstly, we analyze the probability distributions of the logarithmic returns and the cumulative distributions of the normalized price returns for the actual data (SSE composite index, SZSE composite index, DJIA, IXIC, S&P500), and for the financial model with the different finite range values R, when $\lambda = 10, n = 400, \theta = 0.1$ in Fig. 3 and Table 3.

R is the range of the financial model. In Fig. 3 and Table 3, the comparisons of the statistical properties for the real markets and the model are given, and we can see that the fat-tails phenomena is more obviously with R increasing. It can be explained that the interaction among the individuals becomes more actively, because the information spreads more widely in the finite range contact model when the value of R increases, which shows that the model is in accord with the real markets to some extent. In addition, all the four plots in the above Fig. 3 show that, the tails behaviors of the larger range contact model (with $R = 3$) is the closest to that of the actual data (SSE composite index) among the three ranges contact models. In Table 3, we also can obtain that the kurtosis of the contact model with $R = 3$ is closer to real markets than the others.

Secondly, we investigate the statistical properties of the returns for the different intensity values $\lambda \cdot \lambda$ stands for the spread rate of the investment information. The fat-tails and the peak phenomenon of the logarithmic returns are more evidently with the value of λ increasing in Fig. 4 and Table 4. For the fixed other three parameters ($R = 3, n = 729$ and $\theta = 0.01$), the returns of the model is fluctuating more greatly as the intensity value λ is increasing. This is because that the larger the

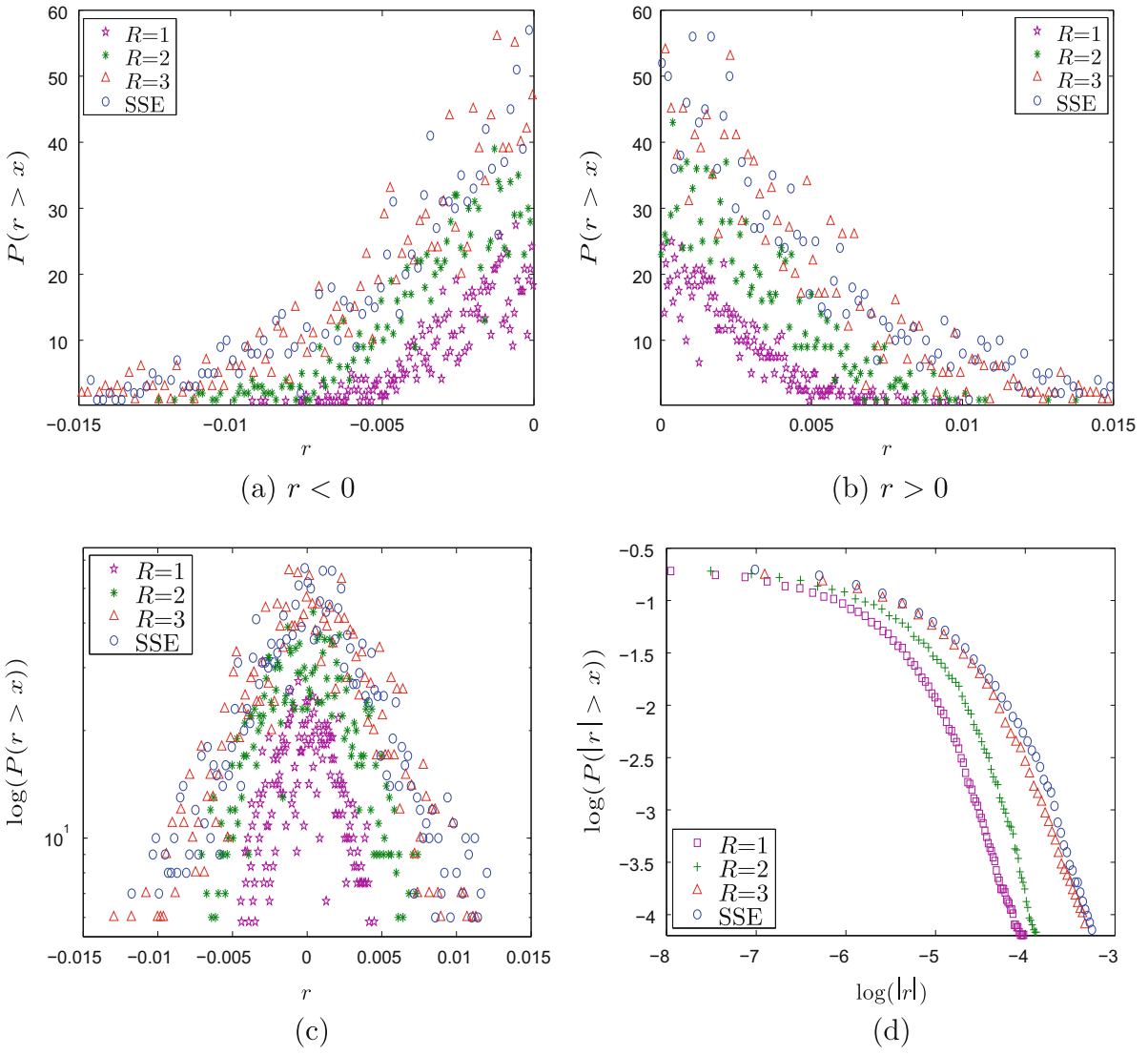

Fig. 3. The plots (a)–(c) are the probability distributions of the logarithmic returns, and the plot (d) is the cumulative distributions of the normalized price returns. The data is selected from SSE composite index and from the simulation data with the different values of R when $\lambda = 10, n = 400, \theta = 0.1$.

Table 3
The statistics of returns for the ranges R.

	Kurtosis	Skewness	Variance	Mean	Max	Min
$R = 1$	3.0358	−0.0668	1.3518e−005	−6.2020e−005	0.0138	−0.0124
$R = 2$	3.1417	0.0319	7.3156e−006	−4.0196e−005	0.0099	−0.0093
$R = 3$	6.1434	−0.1672	3.7557e−005	−5.3405e−005	0.0396	−0.0387
SSE	8.3781	−0.1473	5.1425e−005	9.6897e−005	0.0476	−0.0411
SZSE	8.0379	−0.3793	5.6844e−005	9.3921e−005	0.0476	−0.0446
DJI	11.7555	−0.0947	2.3641e−005	9.9449e−005	0.0456	−0.0356
IXIC	7.8925	−0.1435	6.7744e−005	6.8041e−005	0.0492	−0.0568
S&P500	12.0694	−0.1908	2.6935e−005	8.7280e−005	0.0476	−0.0411

proportion of individuals knowing the information is, the more possibly the information spreads widely. Additionally, it is known that the kurtosis of the Gaussian distribution is 3. From Tables 3 and 4, for both the real markets and the model, all the kurtosis are lager than 3. Moreover, the above results show that the returns of the model becomes more closely to the actual data (SSE composite index) when λ increasing.

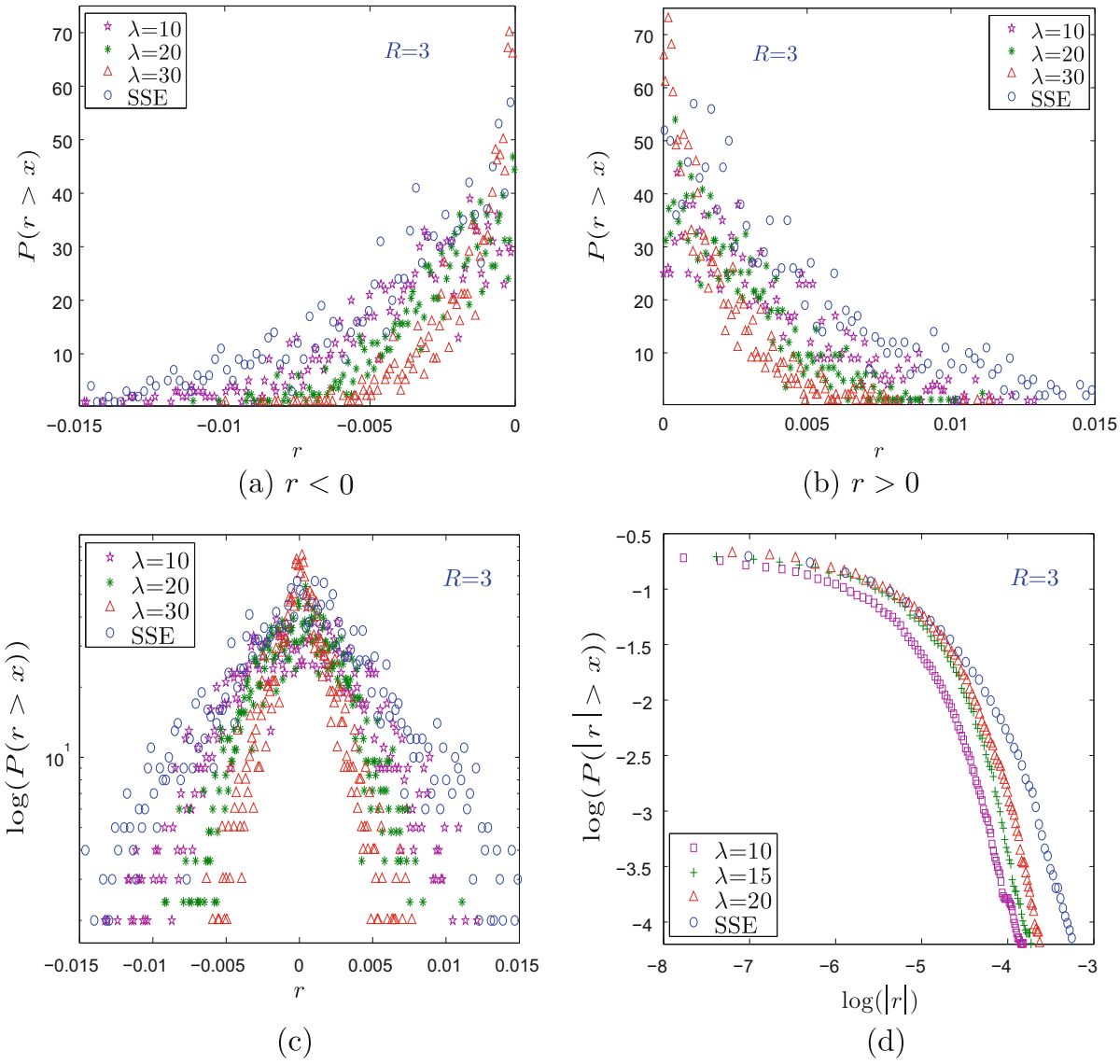

Fig. 4. The plots (a)–(c) are the probability distributions of the logarithmic returns, and the plot (d) is the cumulative distributions of the normalized price returns. The data is selected from SSE and the simulation data with the different values of λ when $R = 3, n = 729, \theta = 0.01$. The fat-tails and the peak phenomenon of the returns are more evidently when the value λ increases.

Table 4
The statistics of returns for the values λ.

R	λ	Kurtosis	Skewness	Variance	Mean	Max	Min
1	10	2.9992	−0.0513	1.3476e−005	−2.5957e−005	0.0123	−0.0148
1	15	3.0352	−0.0868	1.6231e−005	−3.8236e−006	0.0135	−0.0140
1	20	3.1122	−0.0142	1.5202e−005	9.6272e−005	0.0149	−0.0139
2	10	3.0718	0.0541	7.3075e−006	−2.9064e−005	0.0099	−0.0093
2	15	3.1584	0.0828	8.9720e−008	1.7949e−006	0.0011	−0.0011
2	20	3.1859	−0.0133	6.4147e−008	5.4222e−006	0.0010	−8.9545e−004
3	10	3.0566	−0.1275	3.7346e−005	−7.0893e−005	0.0396	−0.0387
3	15	3.0985	0.0048	5.9147e−008	−1.8920e−006	8.3404e−004	−0.0011
3	20	5.8741	0.0042	4.1764e−008	3.5743e−007	7.7446e−004	−7.7585e−004

Remark. In the present paper, the financial model is considered only for the range $R = 1, 2, 3$ and some parameter settings. The phenomena that most of our results of the financial model are on the left sides of the actual SSE data, see Figs. 3(d), 4(d) and 5(d). In fact, this is caused by the parameter setting. If the parameter setting is properly changed, the result of the

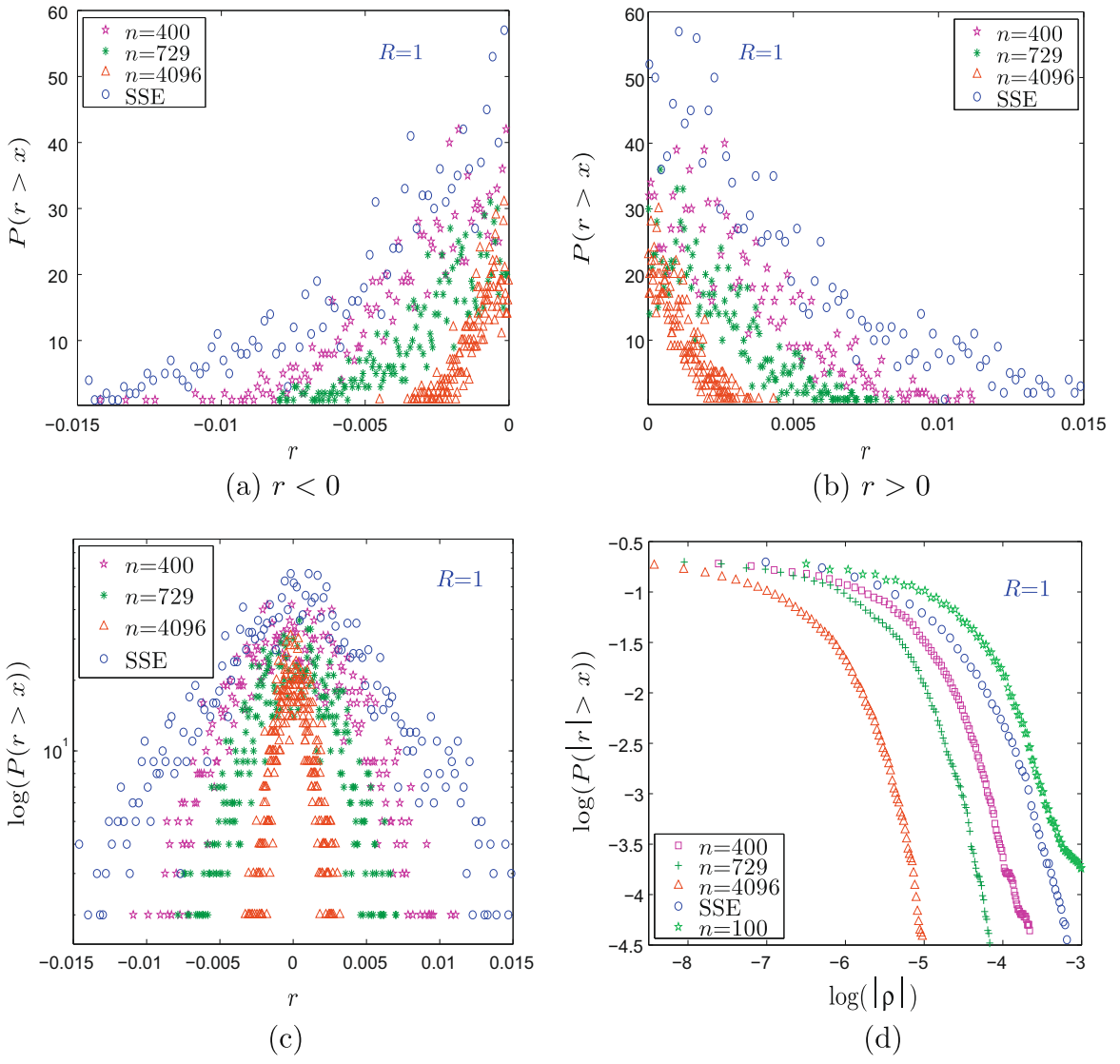

Fig. 5. The plots (a)–(c) are the probability distributions of the logarithmic returns, and the plot (d) represents the cumulative distributions of the normalized price returns. The data is selected from SSE composite index and the simulation data with the different numbers of n when $R = 1, \lambda = 10, \theta = 0.1$.

Table 5
The statistics of returns for the numbers n.

R	n	Kurtosis	Skewness	Variance	Mean	Max	Min
1	400	3.5992	−0.0513	1.3476e−005	−2.5957e−005	0.0123	−0.0148
1	729	3.1934	−0.0195	7.8010e−006	9.6512e−006	0.0112	−0.0092
1	4096	3.0040	0.0067	1.3565e−006	−1.2833e−005	0.0043	−0.0045
(R, λ, θ)	n						
(1,6,0.1)	10000	2.8439	−0.0915	3.3561e−007	1.2450e−006	0.0018	−0.0020
(1,7,0.1)	10000	3.0341	0.0600	3.9358e−007	−1.2001e−005	0.0025	−0.0021
(1,8,0.1)	10000	3.0366	0.0129	4.1927e−007	−1.1876e−006	0.0026	−0.0023
(1,9,0.1)	10000	3.0449	−0.0827	4.9385e−007	6.6975e−006	0.0023	−0.0025
(1,10,0.1)	10000	3.1206	−0.1224	5.5810e−007	2.0803e−006	0.0024	−0.0028

financial model can be on the right side of the actual SSE data. For example for $R = 1, \lambda = 10, \theta = 0.1, n = 100$, the plot of the model appears on the right side the actual SSE data, see Fig. 5(d).

Thirdly, we study the statistical properties of the returns for the different investor numbers n, which stands for the size of investment in the stock market. For the fixed values $R = 1$, $\lambda = 10$ and $\theta = 0.1$, the behavior of the price changes is becoming more closely to that of the actual data (SSE composite index) when n decreasing. In (d) of Fig. 5, we can see that the tails distributions of the simulative data deviate from that of the actual data with n increasing. In Table 5, the kurtosis value decreases with n increasing. It shows that, when the size of investment becomes larger in a stock market, the fluctuation degrees of the market will be weakened.

Remark. Because the number of investors is very large in the real stock markets, we investigate the statistical properties of returns for different values λ, when n is set to 10,000 and $R = 1, \theta = 0.1$ in Table 5. The number of simulation data from the financial model is about 3000. The result is similar as before. For the fixed three parameters $R = 1, n = 10,000$ and $\theta = 0.1$, the returns of the model fluctuate more greatly as the intensity value λ increases. This is because that the larger the proportion of individuals knowing the information is, the more possibly the information spreads widely.

Finally, we discuss the statistical behaviors of the returns for the different values θ, which is the initial density of the financial model and denotes the proportion of individuals knowing the information at the beginning of each trading day. Similarly to the above figures, we can plot the similar graphs of the probability distributions and the power-law distributions for the returns. Here we only give the statistics of the returns for the value θ in Table 6. For the fixed values $R = 2, \lambda = 10$ and $n = 729$, the value of kurtosis increases with θ increasing, and the value is larger than 3. The peak phenomenon is more distinctly with θ increasing, this is because that the larger the proportion of individuals knowing the information at the beginning of each trading day is, the more possibly the information spreads widely.

4.3. Individual stocks of large-cap, mid-cap and small-cap and simulation in financial crisis period

The companies listed in a stock market are categorized as small-cap (small-capitalization), mid-cap or large-cap, which is a measure by which we can classify a company's size. It is important for investors to gauging a company's size and riskiness. The value of market capitalization for a company is calculated by multiplying the number of a company's outstanding shares by its current stock price.

In the present paper, six individual Chinese stocks from large-cap (DQTL, CRCC), mid-cap (YYTM, BLGF) and small-cap (AXXT, SITI) categories are selected and analyzed in Table 7. All of the six stocks are barometer stocks in their fields in

Table 6
The statistics of returns for the values θ.

R	θ	Kurtosis	Skewness	Variance	Mean	Max	Min
1	0.05	2.9309	−0.0783	1.0124e−005	2.9463e−005	0.0110	−0.0113
1	0.10	2.9986	−0.0513	1.3479e−005	−2.5940e−005	0.0123	−0.0148
1	0.15	2.8753	−0.0238	1.2108e−005	−2.9010e−006	0.0112	−0.0123
1	0.20	3.0456	−0.0834	8.6045e−006	7.1291e−006	0.0102	−0.0117
1	0.30	3.1996	−0.0187	3.5583e−006	−6.4251e−006	0.0073	−0.0077
1	0.40	3.5736	−0.0827	1.5440e−006	−2.3807e−005	0.0050	−0.0064
2	0.05	3.0143	0.0454	1.2858e−007	1.7847e−006	0.0015	−0.0013
2	0.10	3.0353	0.0150	1.3101e−007	−5.5284e−006	0.0014	−0.0018
2	0.15	2.9522	0.0169	1.3174e−007	−5.5405e−006	0.0013	−0.0014
2	0.20	3.1803	−0.0411	6.2740e−008	8.3316e−007	8.3404e−004	−8.9545e−004
2	0.30	3.2083	0.0182	6.6719e−008	2.7130e−006	0.0011	−8.3564e−004
3	0.05	2.9668	0.0277	8.6576e−008	−4.0573e−006	0.0010	−0.0011
3	0.10	3.1521	0.0091	8.7355e−008	3.8884e−007	9.5318e−004	−0.0011
3	0.15	2.9732	−0.0424	8.6716e−008	2.3554e−006	0.0011	−0.0013
3	0.20	3.2098	0.0274	8.7445e−008	−3.9990e−006	0.0011	−0.0011
3	0.30	3.5408	0.0060	8.6982e−008	1.1279e−006	0.0012	−9.5528e−004

Table 7
Individual stocks from large-cap, mid-cap and small-cap categories.

	Kurtosis	Skewness	Variance	Mean	Max	Min	Mkt. Cap (RMB)
DQTL	3.9236	−0.1105	2.0768e−004	3.7296e−004	0.0416	−0.0459	140.928B
CRCC	4.9189	−0.2768	1.5109e−004	−2.6174e−004	0.0416	−0.0457	112.642B
YYTM	7.0331	−0.5748	2.3529e−004	6.4365e−004	0.0415	−0.1266	18.494B
BLGF	5.7343	−0.2338	1.5936e−004	9.7315e−005	0.0416	−0.0857	17.660B
AXXT	7.1864	−0.1637	2.2291e−004	1.4767e−004	0.0951	−0.1243	7.554B
SITI	6.8929	−0.3816	2.3093e−004	4.1380e−005	0.0419	−0.1334	4.167B
(R, λ, n, θ)							
(1, 20, 300, 0.15)	3.9085	−0.0264	8.2392e−006	1.1512e−004	0.0120	−0.0117	
(3, 10, 400, 0.1)	6.1434	−0.1672	3.7557e−005	−5.3405e−005	0.0396	−0.0387	

Table 8
Statistical behaviors during the financial crisis period (from September 2008 to August 2009).

	Kurtosis	Skewness	Variance	Mean	Max	Min
SSE	4.4356	0.0961	9.8319e−005	6.3622e−004	0.0392	−0.0284
SZSE	4.1460	−0.4031	1.0524e−004	0.0010	0.0370	−0.0308
DJI	5.5665	0.0570	1.0258e−004	−1.6656e−004	0.0456	−0.0356
IXIC	4.2055	−0.0249	1.6926e−004	−4.8810e−004	0.0485	−0.0416
S&P500	4.5495	−0.0438	1.7035e−004	−6.5333e−004	0.0476	−0.0411
(R, λ, n, θ)						
(1, 20, 300, 0.15)	3.9085	−0.0264	8.2392e−006	1.1512e−004	0.0120	−0.0117
(1, 20, 200, 0.15)	4.7226	0.0943	1.0084e−005	1.5101e−005	0.0148	−0.0151
(1, 20, 100, 0.15)	5.9930	0.0624	1.4674e−005	3.8852e−005	0.0182	−0.0176

Chinese stock markets. In the same category, the statistics of returns for the stocks exhibits the similar statistical behaviors. The kurtosis of DQTL and CRCC from the large-cap categories are 3.9236 and 4.9189, respectively, and smaller than those of stocks from mid-cap (7.0331 and 5.7343) and small-cap (7.1864 and 6.8929) categories. In addition, we find that the statistics of the financial model is close to that of large-cap (DQTL, CRCC) and small-cap (AXXT, SITI) categories with $\{R = 1, \lambda = 20, n = 300, \theta = 0.15\}$ and $\{R = 3, \lambda = 10, n = 400, \theta = 0.1\}$, respectively. Table 7 implies that the classification of companies into different caps also allows investors to gauge the growth versus risk potential, since it usually appeared that large-caps have experienced slower growth with lower risk, meanwhile, small-caps have experienced higher growth potential, but with higher risk.

Next, we analyze and compare the statistical properties of the actual data (SSE composite index, SZSE composite index, DJIA, IXIC, S&P500) during the financial crisis period from September 2008 to August 2009 in Table 8. We can find that the statistics of returns for the five indices are similar, and the values of kurtosis are among in the interval (4, 6). This shows that Chinese stock markets have the similar behaviors to the foreign stock markets during the financial crisis. And the comparisons of returns for the five indices and the financial price model are also given in Table 8, where the parameter settings for the financial model are $\{R = 1, \lambda = 20, n = 100, \theta = 0.15\}, \{R = 1, \lambda = 20, n = 200, \theta = 0.15\}$ and $\{R = 1, \lambda = 20, n = 300, \theta = 0.15\}$.

In summary, R is the range of the financial model. The fat-tails phenomena is more obviously with R increasing. It can be explained that the interaction among the individuals becomes more actively, because the information spreads more widely in the finite range contact model when the value of R increases. λ stands for the spread rate of the investment information. The fat-tails and the peak phenomenon of the logarithmic returns are more evidently with the value of λ increasing. This is because that the larger the proportion of individuals knowing the information is, the more possibly the information spreads widely. n, the investor numbers, is the size of investment in the stock market. The fat-tails phenomena is less obviously with n increasing. This can be explained that when the size of investment becomes larger in a stock market, the fluctuation degrees of the market will be weakened. θ is the initial density of the financial model and denotes the proportion of individuals knowing the information at the beginning of each trading day. The peak phenomenon is more distinctly with θ increasing, this is because that the larger the proportion of individuals knowing the information at the beginning of each trading day is, the more possibly the information spreads widely.

5. The long range correlations of the returns by the detrended fluctuation analysis

The objective of this section is to investigate the long range power-law correlations in the returns time series, and the detrended fluctuation analysis (DFA) method is applied in this work, see [4,5,15]. The DFA is a technique used to estimate a scaling exponent from the behavior of the average fluctuation of a random variable around its local trend. We consider a time series $x(t), t = 1, \ldots, N$, then the integrate time series $y(k)$ is given by

$$y(k) = \sum_{t=l}^{k} \left[x(t) - \frac{1}{N} \sum_{k=1}^{N} x(t) \right].$$

The integrate time series is divided into intervals of equal size, m. In each interval, a polynomial function $y_{fit}(t)$ is fitted to the data. For a given interval size m, the root mean square fluctuation is introduced as follows

$$F(m) = \sqrt{\frac{1}{N} \sum_{t=1}^{N} [y(t) - y_{fit}(t)]^2}.$$

The above definition is repeated for all the divided intervals. There is a power-law relation between $F(m)$ and the interval size m indicates the presence of a scaling: $F(m) \propto m^{\alpha}$. The parameter α is the scaling exponent or the correlation exponent, which denotes the long range power-law correlations of the time series. For the value $\alpha = 0.5$, it indicates that the time series is uncorrelated (white noise); for the value $0 < \alpha < 0.5$, it indicates the power-law anticorrelations; for $0.5 < \alpha < 1$, the time

series has the persistent long range power-law correlations; for $\alpha > 1$, it indicates that the correlations exist but not in a power-law form. Next, by applying the DFA analysis, we study the behaviors of the returns for the SSE composite index and the simulation data with the different values of $\lambda(\lambda = 10, 15, 20)$ and $R(R = 1, R = 2, R = 3)$ in Fig. 6 and Table 5.

The above research work is used to measure correlations in high frequency financial time series. In Fig. 6 and Table 9, it can be seen that the distribution of $F(t)$ for the simulative data is approaching to the SSE composite index when λ is increasing. Further, Table 9 shows the statistical analysis of the scaling exponents for the returns. All of the exponents are very close to 0.5, this shows that there is no strong indication of the long range power-law correlations for the returns.

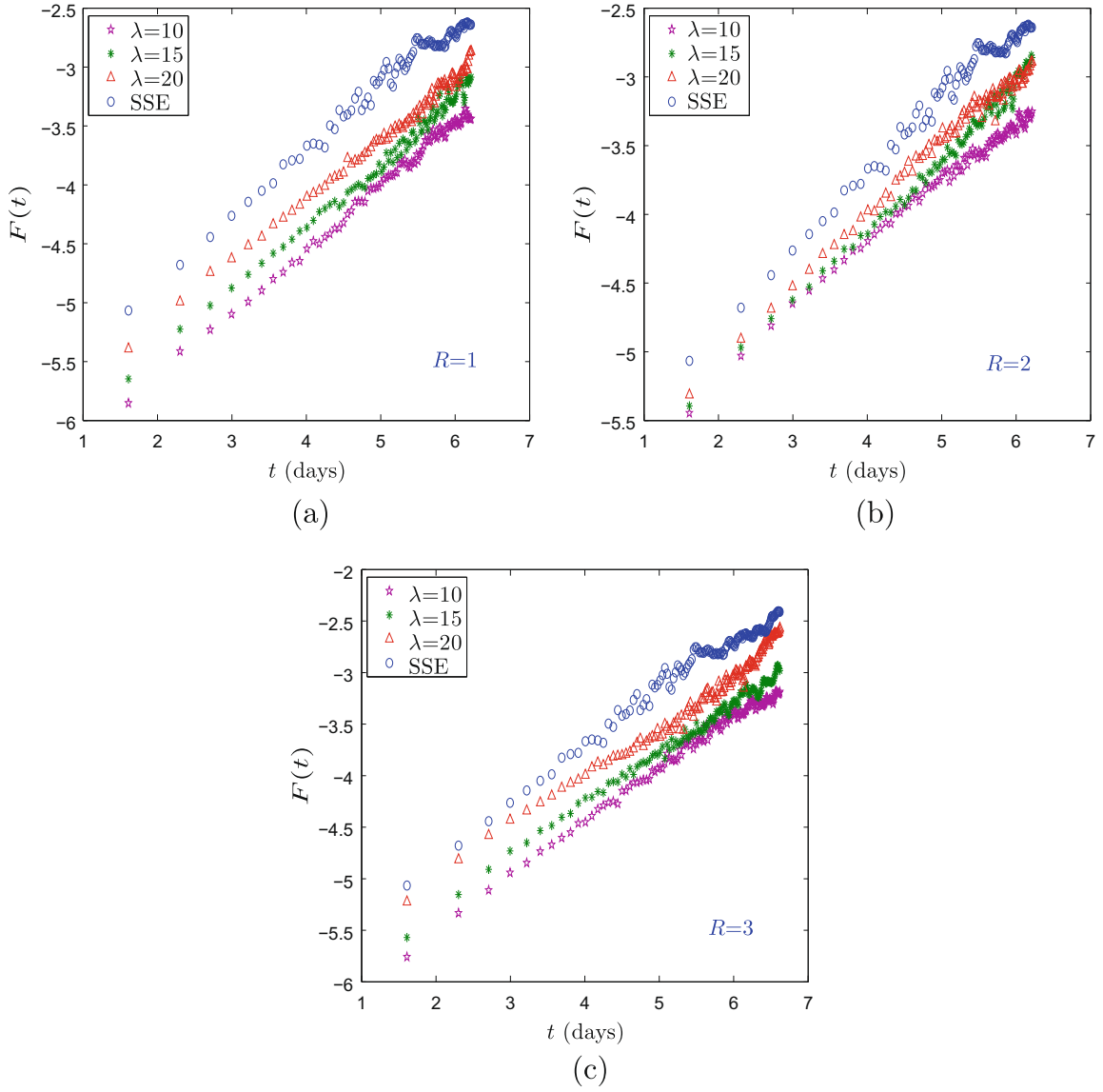

Fig. 6. DFA analysis of the returns for the SSE and the simulation data. (a) $R = 1, n = 400, \theta = 0.1$ with the different values of $\lambda(\lambda = 10, 15, 20)$; (b) $R = 2, n = 729, \theta = 0.1$ with the different values of λ; (c) $R = 3, n = 729, \theta = 0.01$ with the different values of λ.

Table 9
DFA test statistics of the returns.

	$R = 1, \lambda = 10$	$R = 1, \lambda = 15$	$R = 1, \lambda = 20$	$R = 2, \lambda = 10$	$R = 2, \lambda = 15$
α	0.3643	0.5134	0.4502	0.4605	0.4781
	$R = 2, \lambda = 20$	$R = 3, \lambda = 10$	$R = 3, \lambda = 15$	$R = 3, \lambda = 20$	*SSE*
α	0.4463	0.4032	0.4223	0.4931	0.4883

6. The analysis of the data by the q-Gaussian dynamic system

In this section, we apply q-Gaussian distribution to describe and compare the positive part of the probability distribution of the logarithmic returns for the actual data and the simulation data. Tsallis statistics or nonextensive statistical mechanics, a generalization of ordinary Boltzmann–Gibbs statistical mechanics, is used to describe the statistical behaviors of complex systems. The q-Gaussian distribution is a generalized canonical distribution and its typical realization, see [19].

We consider the Brownian particle, whose velocity is u, and it satisfies the following Langevin equation

$$\dot{u} = -\gamma u + \sigma L(t)$$

where $L(t)$ is a Gaussian white noise with $E(L(t)) = 0$ and $E(L(t_1)L(t_2)) = 2\delta(t_1 - t_2)$, γ is a friction positive constant, and σ the strength of $L(t)$. Let $\beta = \gamma/\sigma^2$, and suppose that β follows the $\chi^2(2\alpha)$ distribution. The probability density of β is given by

$$f(\beta) = \frac{1}{\Gamma(\alpha)}\left(\frac{\alpha}{\beta_0}\right)^{\alpha}\beta^{\alpha-1}\exp\left\{\frac{-\alpha\beta}{\beta_0}\right\}$$

where $\alpha > 2, \beta_0 > 0$. Then under some conditions (see [17]), we have the distribution of u is given by

$$p(u) = \frac{\Gamma\left(\alpha+\frac{1}{2}\right)}{\Gamma(\alpha)}\left(\frac{\beta_0}{2\pi\alpha}\right)^{\frac{1}{2}}\left(1+\frac{\beta_0}{2\alpha}u^2\right)^{-\alpha-\frac{1}{2}}$$

where $E(\beta) = \beta_0$. This generates the following q-Gaussian distribution

$$p(u) \propto (1+\beta^*(q-1)u^2)^{-\frac{1}{q-1}}$$

where β^* is a constant. Because β follows χ^2-distribution, then $T = 1/\beta$ is the inverse χ^2-distribution

$$f_T(T) = \frac{1}{\Gamma(\alpha)}(\alpha T_0)^{\alpha}T^{-(1-\alpha)}\exp\left\{-\frac{\alpha T_0}{T}\right\}$$

where T_0 is the mean of T. Because there are some offset along the vertical axis in the plots, an offset is added to the above equation. Then we have

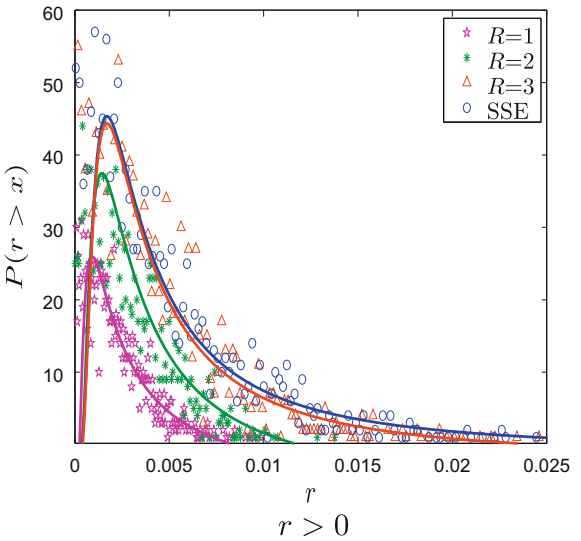

Fig. 7. The probability distributions of the logarithmic returns with the different ranges of R when $\lambda = 10, n = 400$ and $\theta = 0.1$. And the plots of the corresponding scaled $g_T(T)$.

Table 10
The statistics of the returns for the ranges R.

	α	T_0	σ
$R = 1$	0.3 ± 0.1	0.0045 ± 0.0001	17.4 ± 0.1
$R = 2$	0.6 ± 0.1	0.0038 ± 0.0001	17.4 ± 0.1
$R = 3$	0.8 ± 0.1	0.0038 ± 0.0001	5.4 ± 0.1
SSE	0.8 ± 0.1	0.0038 ± 0.0001	2.9 ± 0.1

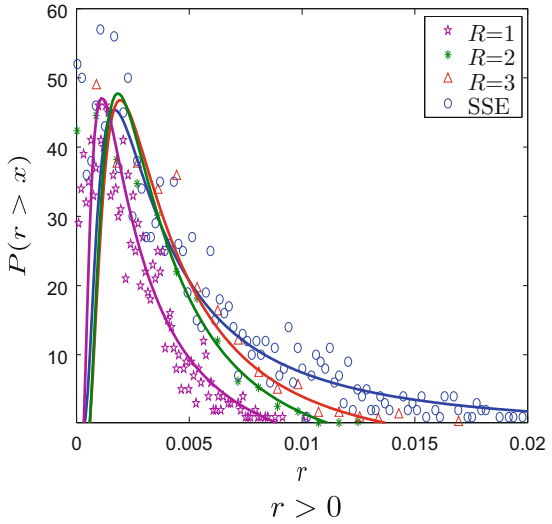

Fig. 8. The probability distributions of the logarithmic returns with the different ranges of R when $\lambda = 10, n = 729$ and $\theta = 0.2$. And the plots of the corresponding scaled $g_T(T)$.

Table 11
The statistics of the returns for the ranges R.

	α	T_0	σ
$R = 1$	0.6 ± 0.1	0.0030 ± 0.0001	20.3 ± 0.1
$R = 2$	1.1 ± 0.1	0.0035 ± 0.0001	20.3 ± 0.1
$R = 3$	1.1 ± 0.1	0.0037 ± 0.0001	14.5 ± 0.1
SSE	0.8 ± 0.1	0.0038 ± 0.0001	2.9 ± 0.1

$$g_T(T) = f_T(T) - \sigma.$$

We discuss the positive part of the probability distributions of the logarithmic returns for the actual data and the simulation data for the different values of R when $\lambda = 10$, $n = 400$ and $\theta = 0.1$ in Fig. 7 and Table 10, and when $\lambda = 10, n = 729$ and $\theta = 0.2$ in Fig. 8 and Table 11. In Figs. 7 and 8, the plots of the scaled $g_T(T)$ is given by $g_T(T)/2.9$, and we find that the function $g_T(T)$ can be approximately identified with the stock market volatilities and the finite range contact model. In Tables 10 and 11, α is becoming larger while T_0 is becoming smaller with R increasing. Additionally, the curve generated by the function $g_T(T)$ to describe the simulation data is closing to that to describe the actual data (SSE composite index) with the value of R increasing. Especially, the curve for simulation data when $R = 3$ is the nearest to the tails distribution of SSE composite index.

7. Conclusion

In the present paper, a new random stock price model of stock markets based on the finite range contact process is modeled. For the different values of the range R, through the computer simulation and the statistical analysis, the behaviors of the financial model are investigated and analyzed. And the comparisons of the indices returns for SSE, SZSE, DJIA, IXIC, S&P500 and the financial model are given. Further, the individual Chinese stocks from large-cap, mid-cap and small-cap categories are discussed, and the fluctuations of the above stock indices are also studied during the financial crisis period. The results show that these indices and individual stocks have the fat-tails phenomena, the power-law distributions, but there is no strong indication of the long range power-law correlations for these returns. At last, the positive parts of the probability distributions of the logarithmic returns for the actual data and the simulation data are compared by the q-Gaussian distribution. All the results show that the stock price model is accord with the real stock market to some degree.

Acknowledgements

The authors were supported in part by National Natural Science Foundation of China Grant Nos. 70771006 and 10971010, BJTU Foundation No. 2006XM044.

References

[1] F. Black, M. Scholes, The pricing of options and corporate liabilities, Journal of Political Economy 81 (1973) 637–654.
[2] U. Divakaran, A. Dutta, Long-range connections, quantum magnets and dilute contact processes, Physica A 384 (2007) 39–43.
[3] R. Gaylord, P. Wellin, Computer Simulations with Mathematica: Explorations in the Physical, Biological and Social Science, Springer-Verlag, New York, 1995.
[4] P. Grau-Carles, Long-range power-law correlations in stock returns, Physica A 299 (2001) 521–527.
[5] K. Hu, P. Ivanov, Z. Chen, P. Carpena, H.E. Stanley, Effect of trends on detrended fluctuation analysis, Physical Review E 64 (2001) 011114.
[6] K. Ilinski, Physics of Finance: Gauge Modeling in Non-equilibrium Pricing, John Wiley, New York, 2001.
[7] G. Iori, A threshold model for stock return volatility and trading volume, International Journal of Theoretical and Applied Finance 3 (2000) 467–472.
[8] N. Konno, Lecture Notes on Interacting Particle Systems, Rokko Lectures in Mathematics, Kobe University, Kobe, 1997.
[9] A. Krawiecki, Microscopic spin model for the stock market with attractor bubbling and heterogeneous agents, International Journal of Modern Physics C 16 (2005) 549–559.
[10] D. Lamberton, B. Lapeyre, Introduction to Stochastic Calculus Applied to Finance, Chapman and Hall/CRC, London, 2000.
[11] Q. Li, J. Wang, Statistical properties of waiting times and returns in Chinese stock markets, WSEAS Transactions on Business and Economics 3 (2006) 758–765.
[12] Z. Liao, J. Wang, Forecasting model of global stock index by stochastic time effective neural network, Expert Systems with Applications 37 (2010) 834–841.
[13] T.M. Liggett, Interacting Particle Systems, Springer-Verlag, New York, 1985.
[14] T.M. Liggett, Stochastic Interacting Systems: Contact, Voter and Exclusion Processes, Springer-Verlag, Berlin, Heidelberg, 1999.
[15] D. Pirino, Jump detection and long range dependence, Physica A 388 (2009) 1150–1156.
[16] V. Plerou, P. Gopikrishnan, B. Rosenow, L.A.N. Amaral, H.E. Stanley, Econophysics: financial time series from a statistical physics point of view, Physica A 279 (2000) 443–456.
[17] D. Stauffer, N. Jan, Sharp peaks in the percolation model for stock markets, Physica A 277 (2000) 215–219.
[18] H. Tanaka, A percolation model of stock price fluctuations, Mathematical Economics 1264 (2002) 203–218.
[19] C. Tsallis, R. Mendes, A. Plastino, The role of constraints within generalized nonextensive statistics, Physica A 261 (1998) 534–554.
[20] J. Wang, Stochastic Process and Its Application in Finance, Tsinghua University Press and Beijing Jiaotong University Press, Beijing, 2007.